Available online at www.sciencedirect.com
ScienceDirect
Journal of Power Sources 161 (2006) 901–906
JOURNAL OF POWER SOURCES
www.elsevier.com/locate/jpowsour

Novel compressive seals for solid oxide fuel cells

Shiru Le [a], Kening Sun [a,*], Naiqing Zhang [a,b], Maozhong An [a], Derui Zhou [a], Jingdong Zhang [c], Donggang Li [c]

[a] *Department of Applied Chemistry, Harbin Institute of Technology, No. 92 West Dazhi Street, P.O. Box 211, 150001 Harbin, PR China*
[b] *The Research Station on Material Science and Engineering for Postoral Fellows No. 2 Yikuang Street, 150001 Harbin, PR China*
[c] *Heilongjiang Provincial Analysis and Testing Center No. 25 of Nantong Street, 150050 Harbin, PR China*

Received 25 March 2006; received in revised form 29 April 2006; accepted 3 May 2006
Available online 7 July 2006

Abstract

Traditional seals for planar solid oxide fuel cells (pSOFCs) are rigid glass and glass–ceramic, which have caused the problem of being unable to replace malfunctioning components. Non-glass sealants have become a recent trend. In this paper, fumed silica-infiltrated alumina–silica fiber paper gaskets were investigated as a novel compressive seal for planar solid oxide fuel cells. The leak rates decreased with increase of the silica-infiltration amount and the compressive load. Samples pre-stressed at 10 MPa indicated far superior sealing characteristics, with leak rates as low as 0.04 sccm cm^{-1} at a 1 MPa compressive stress and a 10 kPa pressure gradient, and 0.05 sccm cm^{-1} for 0.05 MPa, and a 1.4 kPa pressure gradient.

Keywords: SOFC; Compressive seals; Ceramic fiber; Fumed silica

1. Introduction

Planar solid oxide fuel cells (pSOFCs) can provide higher power density than tubular SOFCs, but require high temperature sealants, which are not required in tubular SOFCs. The sealant needs not only to be stable in the dual oxidizing and reducing environments but also has to be electrically insulating and chemically compatible with the other fuel cell components [1,2]. A durable sealant is at or near the top on the list of the many technical hurdles hindering the advance of SOFCs.

So far, most SOFC seal development has focused on boned, rigid seals, which essentially "glue" the stack components together [3–6]—primarily glass and glass–ceramics. The advantage of the rigid seals was that the thermal expansion coefficient (TEC) of the glass–ceramics could be adapted to other stack components by controlling the phase content [3]. However, glass–ceramics were disadvantageous for long-term stack operation, and tended to react with the electrodes and interconnects at the high SOFC operating temperatures [4]. Furthermore, a non-destructive dismantling of the stacks due to malfunctioning components was impossible.

Compressive seals were developed to overcome the disadvantages of rigid glass based seals. The major advantage of compressive seals was that the seals were not rigidly fixed to the other SOFC components, so that an exact match of thermal expansion was not required. This allowed the cells and interconnects to expand freely during thermal cycling and operation, thus, replacement of malfunctioning components became possible. Currently, two kinds of materials are developed for compressive seals: deformable metallic and mica-based seals. Deformable metallic, for example, corrugated or C-shaped gaskets fabricated from superalloys, were designed to maintain high-temperature strength and oxidation resistance to maintain a seal due to the applied pressure [3,7,8]. The best data was obtained in a sandwich arrangement sheet. The leak rate was 0.05 sccm cm^{-1} at 0.7 MPa. However, this was not suitable for SOFC sealing because of the occurrence of short circuits [7,8]. Compressive single layer, multi-layer mica seals or hybrid mica, which added a glass interlayer, have been tested by Chou [9–16]. Systematic investigations have reported the sealing effect of plain mica or hybrid seals. It was noticed that the leak rates decreased sharply with hybrid seals compared to plain mica, and provided the better adaptation of the TEC between adjacent stack components and glass during thermal cycling at 800 °C. However, a compliant glass interlayer was required for the hybrid mica-based seals to reduce the leak rates. The problem of replacing the com-

* Corresponding author. Tel.: +86 451 8641 2153; fax: +86 451 8641 2153.
E-mail address: leshiru2005@yahoo.com.cn (K. Sun).

0378-7753/$ – see front matter © 2006 Elsevier B.V. All rights reserved.
doi:10.1016/j.jpowsour.2006.05.016

Table 1
Physical properties of ceramic fiber [17]

Property	Values
Composition	$Al_2O_3 \geq 45\%$, $SiO_2 \geq 51\%$, $Fe_2O_3 \leq 1.2\%$ $Na_2O + K_2O < 0.5\%$, $TiO_2 < 0.3\%$CaO 1.21%
Diameter (μm)	2–5
Length (mm)	30–250
Porosity	>90%
Volume resistivity at 850 °C (Ω cm)	$>10^6$
Thermal conductivity ($W\,m^{-1}\,K^{-1}$)	~0.0255
Elastic recovery	>93.35%

ponent could not be solved. In boric acid or bismuth nitrate infiltrated-mica, the leak rates tended to increase rapidly after several thermal cycles because of the volatilization of B_2O_3. The objective of the present study is to develop a non-glass compressive seal offering constant or low leak rates (<3% fuel loss) for SOFCs sealing.

Ceramic fiber is an insulation made of an alumina–silica composition. It resists oxidation and is easy to fabricate and install. In addition, it is flexible with an elastic recovery higher than 93.35%. It is widely used in high temperature kilns (normally >1000 °C) for long times, also in furnace insulation and high temperature gaskets. Most of its characteristics meet the demands for SOFC sealing. The physical properties of alumina–silica fiber are listed in Table 1 [17].

However, because its porosity is higher than 90%, infiltration is required for its application to SOFC sealing to reduce leak rates. Selection of an appropriate infiltrant is very important. Apart from effectively reducing the leak rates, the infiltration must be insulating and have chemical stability in the SOFC environment.

In water, fumed silica has a high dispersion and has a chain-like particle morphology forming colloid silica. The fumed silica bond together via weak hydrogen bonds form a three-dimensional network. After drying, the colloid silica with a size much larger than that of fumed silica filled in the voids of the fiber, effectively reducing the leak rates. In this paper, commercially available fumed silica with a particle size of 15–30 nm was chose as the infiltrant. The fumed silica-infiltrated alumina–silica fiber gaskets were used as pSOFC seals initially.

2. Experimental methods

Commercially available alumina–silica fiber paper gaskets of 5 mm thickness were cut into 6 cm × 6 cm pieces with a 2 cm diameter center hole and were then pre-heated at 700 °C for 1 h to burn out the organic binder. Fiber paper was dipped into various concentrations of fumed silica solution for 10 min. The concentration was 50, 100 and 150 g L^{-1} and the weight of fiber paper increased by 38.8, 68.8 and 100 wt.%, respectively. After filling, the fiber paper was totally dried at 80 °C for 8 h before leak testing. To suppress the formation of colloid silica before infiltration, an ultrasonic cleaner was used during infiltrating.

Leak rates of the fiber paper with different infiltrating amounts of fumed silica with and without pre-compression were tested. The pre-compression was 10 MPa for 10 min. Samples were placed between an SS430 cylinder and a SS430 steel plate and then heated to 850 °C. The SS430 cylinder had 2 cm inner diameter and 4 cm outer diameter and was 3 cm in height. A compressive stress of 1–10 MPa or 0.05–0.1 MPa was applied to the cylinder. A 150 cm^3 gas reservoir was kept under ambient conditions and connected to the samples via a 1 mm inner diameter SS430 tube. Two pressures: 1.4 and 15.0 kPa were used. 1.4 kPa is likely to be close to the actual planar SOFC pressure [18] while 15.0 kPa may be considered an upper limit. The line between the nitrogen source and the reservoir was then closed, and the resulting pressure decayed in the reservoir with respect with time from 15.0 to 2.0 kPa or 1.4 kPa to 0. A schematic of the leak rate test is illustrated in Fig. 1. From the pressure decay versus time data, leak rates could subsequently be calculated using the equation [12].

$$L = \frac{(P_i - P_f)V}{P_f\,\Delta t\,C} \quad (1)$$

where L is the leak rate, sccm cm^{-1} (standard cubic centimeter per minute per centimeter), V the reservoir volume and P is the pressure. Subscripts i and f represented the initial and

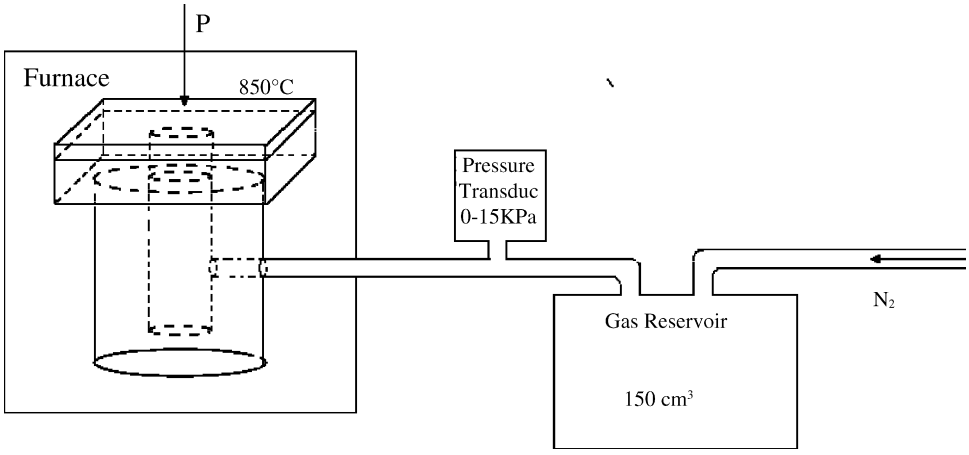

Fig. 1. Schematic of seal testing machine.

final conditions and C is the outer length of the SS430 cylinder circumference (12.56 cm).

The morphology of samples were analyzed by scanning electron microscopy (HITACHI S4700). The chemical stability of the infiltrated ceramic fiber paper and colloid silica were measured by the mass loss in hydrogen at 800 and 850 °C for 20 h.

3. Results and discussion

With different infiltration amounts, leak tests on both samples with and without pre-compression were conducted. The leak rates were expressed as a function of the outer circumference of the cylinder SS430.

3.1. Effect of infiltration on leakage

The effect of infiltration on the leakage is showed in Fig. 2. The leak rates were tested under a 4 MPa compressive load and it was found to be 4.6 sccm cm^{-1} for the ceramic fiber without any infiltration. Under this same condition, 3.5 sccm cm^{-1} (38.8 wt.% infiltration), 1.0 sccm cm^{-1} (68.8 wt.%), 1.0 sccm cm^{-1} (100 wt.%) were found for different infiltrations. It was clear that the leak rates were reduced with increase of the infiltrating amount. From the microstructural examination of the ceramic fiber with and without infiltration in Fig. 3, it was found that the fiber without infiltration interlaced each other as a meshwork, forming 3D leakage paths and leaving spaces in the fiber. The leak rates were high. The infiltrated fumed silica formed colloid silica after drying with the size of most colloid silica being larger than 4 μm, compared with the size of fumed silica was in the range of 15–30 nm. The colloid silica filled in the spaces between fibers, reducing the gap abruptly. These colloid silica fillings then blocked the leakage paths, resulting in lower leakage. However, 1.0 sccm cm^{-1} was still too high for SOFCs sealing.

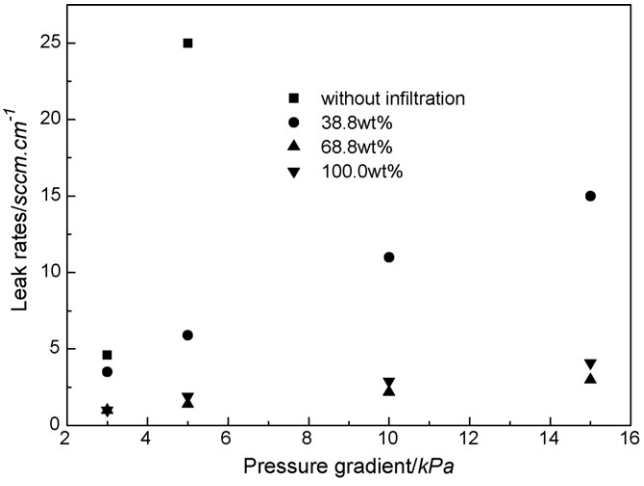

Fig. 2. Effect of infiltration to the leakage at 4 MPa compressive load.

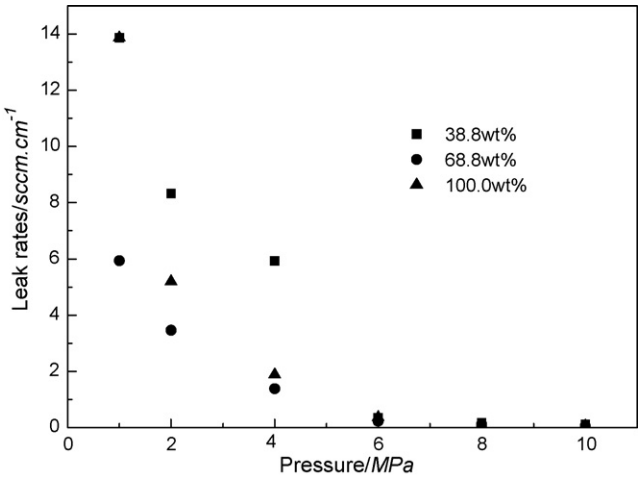

Fig. 4. Leak rates of the samples with different compressive load.

3.2. Effect of compressive load on leakage

The effect of applied compressive load was also investigated. The results are shown in Fig. 4. It is clearly seen that the leakage decreased with the increase of compressive load for all the samples. At a 10 kPa pressure gradient, it was 18.49 sccm cm^{-1} at 1 MPa, compared with 0.11 sccm cm^{-1} at 10 MPa, a 170-fold reduction. This is easily understood, because a more hermetic seal was achieved with higher compressive loads at the interface between the SS430 cylinder and the fiber paper, together with the interface between the fiber paper and the steel plate. Also, higher compressive loads closed the fiber paper. This was evident when the compressive load was increased from 4 to 6 MPa, the leak rates decreased rapidly, this was shown in Fig. 5. For example, for the 38.8 wt.% samples, it was 11.10 sccm cm^{-1} at 4 MPa but

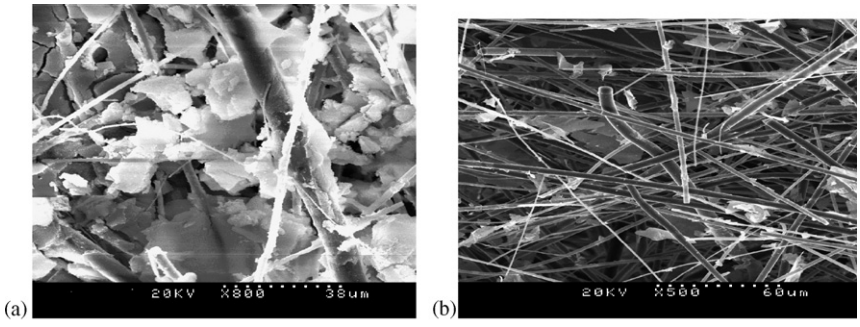

Fig. 3. SEM image of the fiber paper with and without infiltration.

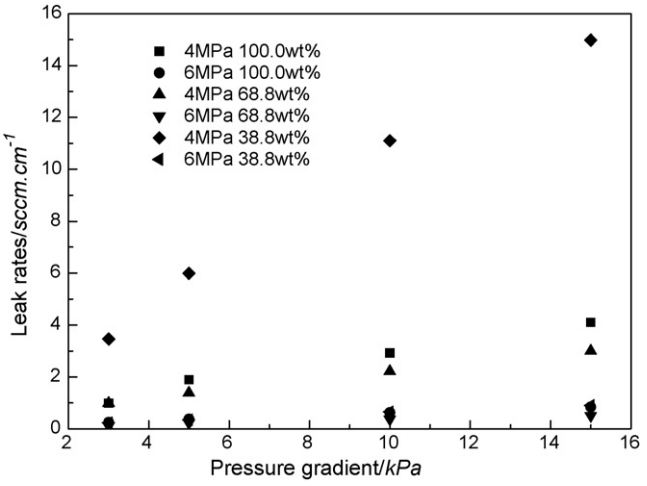

Fig. 5. Leak rates of the samples at 4 and 6 MPa compressive load.

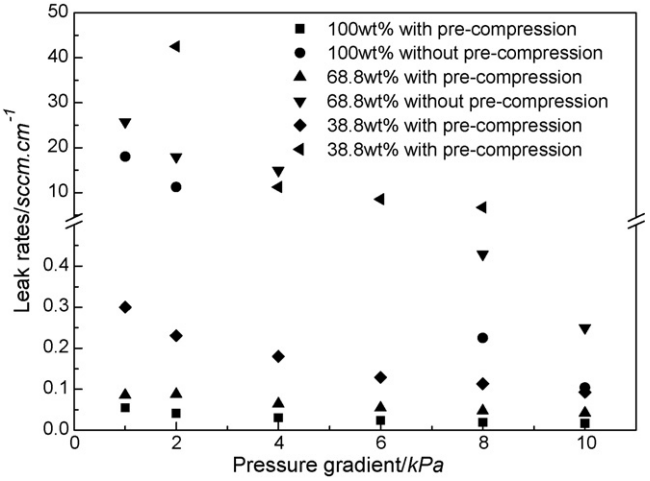

Fig. 6. Leak rates of the samples with and without pre-compression.

was 0.65 sccm cm^{-1} at 6 MPa, i.e. it was reduced about seventeen times. The effect of the compressive load on the leakage was much weaker when the compressive load was higher than 6 MPa. At 8 MPa, for instance, it was 0.31 sccm cm^{-1}, reduced by only one order of magnitude compared with that at 6 MPa. However, 0.65 sccm cm^{-1} at 6 MPa is unacceptable for SOFC sealing.

3.3. Effect of pre-compression

To reduce the leak rates further, a pre-compression method was employed. The leak rates of the samples with and without pre-compression are showed in Fig. 6. It can be seen that the pre-stressed samples indicated far superior sealing characteristics than those without pre-compression, especially at a low compressive load. With a 10 kPa pressure gradient and a 1 MPa compressive load, it was 18.49 sccm cm^{-1} while for 100 wt.% samples with pre-compression, it was only 0.04 sccm cm^{-1}, i.e. reduced by about 460 times. However, the effect of increasing the applied compressive stress was much weaker for the samples with pre-compression. For example, the leak rate was reduced about 50% (from 0.03 to 0.02 sccm cm^{-1}) when the compressive stress increased from 4 to 6 MPa. The fact that the leakage of the pre-stressed samples was less dependent on compressive load also demonstrated that it was more hermetic.

There were two paths for leaks: one was from the interface between the fiber paper and steel cylinder or the interface of ceramic fiber and steel plate; the other was through the fiber itself. SEM images of infiltrated fiber before and after pre-compression in Fig. 7 indicate that there were many cracks in the samples before pre-compression. The colloid could not fill these cracks in the fiber entirely, so leakage occurred through the cracks in the fiber. However, no cracks or holes could be seen in the samples after pre-compression. This demonstrated that the pre-compression would make cracks disappear in the fiber, reducing the leakage. The surface SEM image of the fume-silica infiltrated ceramic fiber with and without pre-compression is shown in Fig. 8. It is evident that there are many cracks in the fiber paper before pre-compression. Because there are long and irregular grooves on the cylinder [12], the colloid with cracks could not hermetically seal the groove. Leakage occurred through the interface. However, the surface of the samples with pre-compression were flat. Few cracks could be seen. This showed that the colloid silica filled most of the grooves and effectively blocked the continuous 3D leak in the interface between the fiber paper and cylinder, and the interface between the ceramic fiber and steel plate.

This finding showed that the pre-compression method effectively reduced the leakage, since it was possible that the alumina–silica fiber could be initially compressed at high load to give improved sealing.

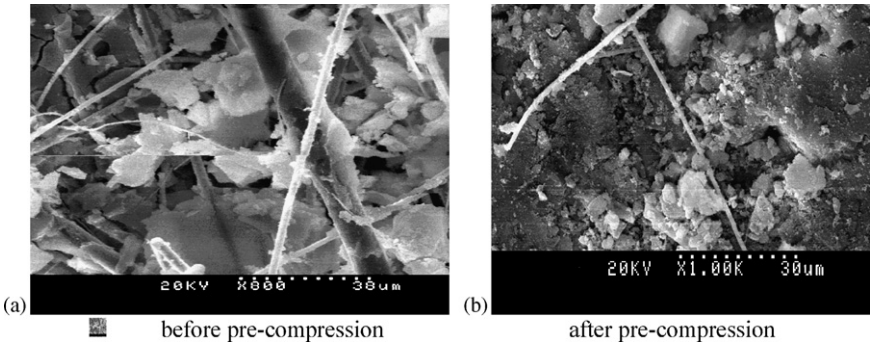

Fig. 7. SEM image in the fiber with and without pre-compression.

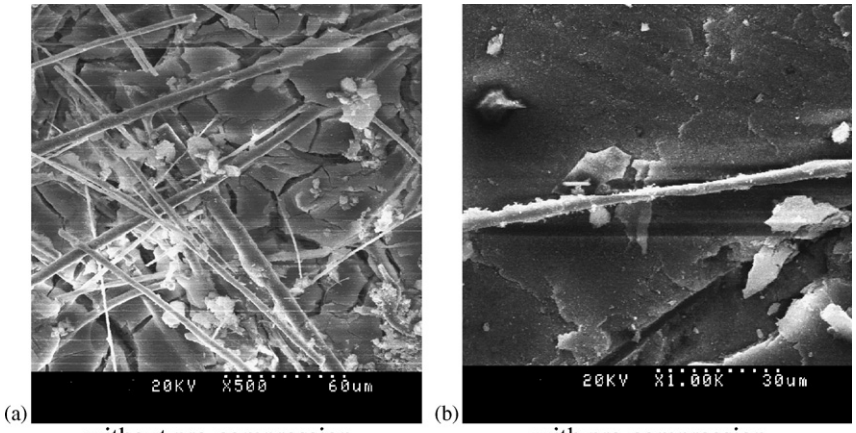

Fig. 8. SEM images of the fiber surface with and without pre-compression.

We also compared the mica-based compressive seals with a 1.4 kPa pressure gradient, which was likely to be similar to the actual planar SOFC conditions. The compressive load was 0.05 MPa (7.35 psi) and 0.1 MPa (14.7 psi). The leak rate was 0.04 sccm cm^{-1} for 100 wt.% sample at 0.05 MPa and 0.03 sccm cm^{-1} at 0.1 MPa. For the glass (20 vol.%)–mica composite, it was 0.04–0.05 sccm cm^{-1} at 0.02 MPa (3 psi) compressive load, 0.011–0.015 sccm cm^{-1} at 0.0827 MPa (12 psi) [16]. For an anode supported SOFC (anode thickness $\geq$1 mm, 10 cm × 10 cm), at 0.05 MPa compressive stress would require 500 N. The PEN would be kept intact at this compressive load (at least in our lab). Though the leak rate was slightly higher for infiltrated fiber than that of glass–mica composite seals, no glass was required.

For the plain muscovite single crystal the leak rate was 0.05 sccm cm^{-1} at 2.07 MPa, 10.3 kPa pressure gradient [12], and for the metal/mica composites compressive seal it was 0.05 sccm cm^{-1} at a 0.7 MPa compressing load, but it was not deemed to be suitable because of short circuits [7,8]. However, it was only 0.03 sccm cm^{-1} at 2 MPa and 0.04 sccm cm^{-1} at 1 MPa of 10 kPa pressure gradient for the fumed silica-infiltrated alumina–silica fiber paper. The leak rates of the fumed silica-infiltrated fiber was only about half that of the plain muscovite SC, and lower than the metal/mica composites seals, so it is a promising compressive seal for SOFC.

To estimate the leakage using these seals in an SOFC stack, we assume that the active area of each cell was $8 \times 8 = 64$ cm^2 with the outer seal length of $4 \times 15 = 60$ cm per cell. The operating current density of 0.7 A cm^2 needed 470 sccm. Considering a fuel utilization of 80%, 584 sccm was required. Assuming a 10.0 kPa pressure gradient (upper limit) across the seal and a leak rate of 0.04 sccm cm^{-1} for the pre-stressed samples with 100 wt.% fumed silica-infiltrated and at 1 MPa compressive load, then the total leakage was only 0.4%.

3.4. Chemical stability

There is concern that as to whether colloid silica and infiltrated ceramic fiber paper are stable in a reducing environment. For colloid silica, the rate of mass was 3.0×10^{-5} g cm^{-2} h^{-1} at 800 °C and 1.2×10^{-4} g cm^{-2} h^{-1} at 850 °C, respectively. For infiltrated ceramic fiber paper, it was 1.5×10^{-5} g cm^{-2} h^{-1} at 800 °C and 8.0×10^{-5} g cm^{-2} h^{-1} at 850 °C. This demonstrates that colloid silica and infiltrated ceramic fiber are stable in a reducing environment. The influence of the mass loss on leak rate will be low because of the low rate of mass loss.

4. Conclusions

Fumed silica-infiltrated alumina–silica fiber paper has shown promising results for planar SOFC compressive sealing. The leak rates decreased with increasing amounts of silica infiltration and under a compressive load. The pre-pressed samples at 10 MPa for 10 min indicated far superior sealing characteristics than those without pre-compression, and the leak rates were as low as 0.04 sccm cm^{-1} with a 1 MPa compressive load, 10 kPa pressure gradient, and 0.05 sccm cm^{-1} at 0.05 MPa compressive load, 1.4 kPa pressure gradient. This was better than plain mica and metal/mica composites seals. The rate of mass loss of colloidally deposited silica and infiltrated ceramic fiber paper was very low at 800 °C.

Acknowledgement

This research was financially supported by the Development for High Technology under contract number 2003AA302440.

References

[1] Q.M. Nguyen, Solid State Ionics 174 (2004) 271–277.
[2] S.C. Singhal, Solid State Ionics 152/153 (2002) 405–410.
[3] W.F. Jeffrey, J. Power Sources 147 (2005) 46–47.
[4] Z.G. Yang, G.G. Xie, K.D. Meinhardt, J. Mater. Eng. Perf. 13 (3) (2004) 327–334.
[5] N. Lahl, D. Bahadur, K. Singh, L. Singheiser, K. Hilpert, J. Electrochem. Soc., 149 (5) (2002) A607–A614.
[6] Z. Yang, J.W. Stevenson, D. Kerry, Solid State Ionics 160 (2003) 213–225.
[7] M. Bram, S. Reckers, P. Drinovac, J. Monch, R.W. Steinbrech, H.P. Buchkremer, D. Stover, Electrochem. Soc. Proc. Vol. 8 (2003) 889–897.
[8] M. Bram, S. Rechers, P. Drinovac, J. Monch, R.W. Steinbrech, H.P. Buchkremer, D. Stover, J. Power Sources 138 (2004) 111–119.
[9] Y.-S. Chou, J.W. Stevenson, J. Power Sources 135 (2004) 72–78.

[10] Y.-S. Chou, J.W. Stevenson, L.A. Chick, J. Power Sources 112 (2002) 130–136.
[11] Y.-S. Chou, J.W. Stevenson, J. Power Sources 124 (2003) 473–478.
[12] Y.-S. Chou, J.W. Stevenson, J. Power Sources 112 (2002) 130–136.
[13] Y.-S. Chou, J.W. Stevenson, J. Power Sources 115 (2003) 274–278.
[14] Y.S. Chou, J.W. Stevenson, L.A. Chick, J. Mater. Res., 18 (2003) 2243–2250.
[15] Z. PLSingh, U. Yang, J.W. Viswanathan, S. tevenson, J. Mater. Eng. Perf. 13 (3) (2003) 287–294.
[16] Y.-S. Chou, J.W. Stevenson, P. Singh, J. Power Sources 152 (2005) 168–174.
[17] Z. Cui, Ceramic Fiber, Chemical Industrial Press, 2004, pp. 28–61.
[18] W. Li, K. Hasinka, M. Seabaugh, S. Swartz, J. Lannutti, J. Power Sources 138 (1/2) (2004) 145–155.